

Algebraic and machine learning approach to hierarchical triple-star stability

Pavan Vynatheya¹, Adrian S. Hamers¹, Rosemary A. Mardling² and Earl P. Bellinger^{1,3}

¹Max-Planck-Institut für Astrophysik, Karl-Schwarzschild-Straße 1, 85748 Garching bei München, Germany

²School of Physics and Astronomy, Monash University, Clayton Victoria 3800, Australia

³Stellar Astrophysics Centre, Department of Physics and Astronomy, Aarhus University, Ny Munkegade 120, Aarhus, Denmark

Accepted XXX. Received YYY; in original form ZZZ

ABSTRACT

We present two approaches to determine the dynamical stability of a hierarchical triple-star system. The first is an improvement on the Mardling-Aarseth stability formula from 2001, where we introduce a dependence on inner orbital eccentricity and improve the dependence on mutual orbital inclination. The second involves a machine learning approach, where we use a multilayer perceptron (MLP) to classify triple-star systems as ‘stable’ and ‘unstable’. To achieve this, we generate a large training data set of 10^6 hierarchical triples using the N -body code MSTAR. Both our approaches perform better than previous stability criteria, with the MLP model performing the best. The improved stability formula and the machine learning model have overall classification accuracies of 93% and 95% respectively. Our MLP model, which accurately predicts the stability of any hierarchical triple-star system within the parameter ranges studied with almost no computation required, is publicly available on Github in the form of an easy-to-use Python script.

Key words: binaries: general – stars: kinematics and dynamics – gravitation

1 INTRODUCTION

The three-body problem has been of interest to physicists ever since classical mechanics was formulated. Unlike the two-body problem, the equations governing the motion of three bodies do not admit general closed-form solutions; the fact that solutions exist that exhibit extreme sensitivity to initial conditions is evidence that this must be true. There are a few specific cases, including the test particle limit or the ‘restricted’ three-body problem, for which closed-form analytic solutions exist, but the general problem can be chaotic and can only be solved numerically. In the past few decades, the advent of computing has vastly improved our knowledge of N -body dynamics.

In this paper, we shall focus on hierarchical triple-star systems. Such a hierarchical configuration can be regarded as two ‘nested’ binaries, with an inner binary of two stars being orbited by a third companion. Unlike isolated binaries, the orbits of a triple can change over periods much greater than orbital timescales, and significantly, depending on the system. This secular evolution in triples leads to, in the lowest-order approximation, von Zeipel-Lidov-Kozai (LK or ZLK) oscillations (von Zeipel 1910; Lidov 1962; Kozai 1962; see Naoz 2016 for a review), which are periodic changes seen in the inner orbital eccentricity and the mutual orbital inclination. Drastic changes in eccentricity can lead to stellar collisions if the orbital periapsis is on the order of stellar size and the LK oscillations are not quenched by general relativistic or tidal effects. Additionally, a large eccentricity can mark the onset of dynamical instability and the subsequent escape of one of the stars.

The physical origin of chaotic behaviour in hierarchical triples involves resonant interactions between the inner orbit and harmonics of the outer orbit (Mardling 2008, 2013). In particular, significant

energy exchange between the orbits must take place for one of the stars to escape, and this can only occur if there is enough power in the harmonic whose frequency is close to the inner orbital frequency. This in turn requires sufficiently high outer eccentricity. As a result, for a particular integer $N \approx P_{\text{out}}/P_{\text{in}}$, it is the $N : 1$ ‘resonance’ and its neighbours which determine stability in triple star systems, with the *resonance overlap stability criterion* from Chirikov (1979) providing a powerful heuristic for assessing this (Mardling 2008). Resonance is at the heart of the simpler Mardling & Aarseth (2001) stability criterion (see Equation 2 below), which is based on the proposal that the ratio of outer to inner semimajor axes is proportional to some power of the ratio of the time of outer periastron passage to the inner orbital period.

Investigating the stability of hierarchical triples is important because of their abundance in the universe. Moe & Di Stefano (2017) found that $\gtrsim 50\%$ of massive O- and B-stars reside in multiple-star systems like triples and quadruples, compared to $\lesssim 10\%$ of solar-mass stars. Hence, the study of massive stars, which includes high-energy phenomena like supernovae and gravitational waves, is incomplete without first understanding the dynamical evolution of triples. However, direct N -body integration is computationally expensive and not always desirable. This makes it necessary to come up with techniques to predict the long-term stability of hierarchical configurations.

Besides being compelling from a pure dynamics perspective, the question of hierarchical triple-star stability is of interest in triple population synthesis studies (e.g., Antonini et al. 2016; Fragione & Loeb 2019). In this context, dynamical stability criteria are an important step in the initial sampling of a population of triple-star systems. A poor classification can impact the statistics of the problem.

In this work, we compare our results to the stability criteria presented by Eggleton & Kiseleva (1995) and Mardling & Aarseth (2001). Eggleton & Kiseleva (1995) proposed an empirical fit for the stability of hierarchical triple-star systems. They assumed a system to be stable if it remains in the same hierarchical configuration after 100 orbits of the ‘outer’ binary. A more widely used stability criterion was provided by Mardling & Aarseth (2001) (see also Mardling & Aarseth 1999). They drew parallels between dynamical instability in triples and tidal evolution and presented a semi-analytical formula to distinguish between stable and unstable systems.

The structure of this paper is as follows. Section 2 briefly describes the N -body code we used and the assumptions we make about stability; Section 3 details the initial conditions and our parameter space; Sections 4 and 5 form the crucial components of this paper, describing our updated stability criterion and our machine learning classifier respectively; Section 6 summarises our results; Section 7 is the discussion; and Section 8 finally concludes. Appendix A provides a brief tutorial to use our machine learning model.

2 N -BODY CODE AND STABILITY

For our study of hierarchical triple-star systems, we use the N -body code MSTAR (see Rantala et al. 2020 for details), which performs highly accurate integration for a wide range of mass ratios. For simplicity, we use the code with the post-Newtonian (PN) terms disabled. The PN terms have little effect when distances are in the order of ~ 1 AU and for stellar-mass scales but can be significant during close encounters and compact object mergers. The reason for ignoring PN terms is to make our problem *scale-free* in mass, distance and time. Thus, we do not need to be concerned about the actual values of masses and distances and instead, concentrate on ratios of quantities.

With the scale-free assumption, hierarchical triple systems have the following relevant initial parameters, which dictate the evolution of the system:

- Inner mass ratio $q_{\text{in}} = m_2/m_1 \leq 1$ ($m_2 \leq m_1$), where m_1 and m_2 are the inner binary masses of the hierarchical triple.
- Outer mass ratio $q_{\text{out}} = m_3/(m_1 + m_2)$, where m_3 is the outer mass of the hierarchical triple.
- Semimajor axis ratio $\alpha = a_{\text{in}}/a_{\text{out}} < 1$, where a_{in} and a_{out} are the semimajor axes of the inner and outer orbits of the hierarchical triple respectively.
 - Inner orbit eccentricity $0 \leq e_{\text{in}} < 1$.
 - Outer orbit eccentricity $0 \leq e_{\text{out}} < 1$.
 - Mutual inclination i_{mut} between the two orbits of the hierarchical triple.

Here, the mutual inclination $\cos(i_{\text{mut}}) = \cos(i_{\text{in}})\cos(i_{\text{out}}) + \sin(i_{\text{in}})\sin(i_{\text{out}})\cos(\Omega_{\text{in}} - \Omega_{\text{out}})$ takes into account two of the three orbit-orientation (Euler) angles, with the inclination i and the longitude of ascending node Ω being defined with respect to a chosen reference direction (the subscripts refer to the inner and outer orbits). In fact, as demonstrated in panels (e) and (f) of Figure 3.16 of Mardling (2008), the stability boundary is also sensitive to the third Euler angle, the argument of periapsis ω , since it is this which determines the position of a system relative to the centre of the relevant $N : 1$ resonance, and as a consequence, the system’s stability. We do not attempt to capture the resulting step-like structure of the stability boundary, instead adopting an expression which effectively smooths this behaviour. Similarly, any dependence on the true anomaly θ is not captured in this work.

We now come to the defining criterion for the stability of a triple.

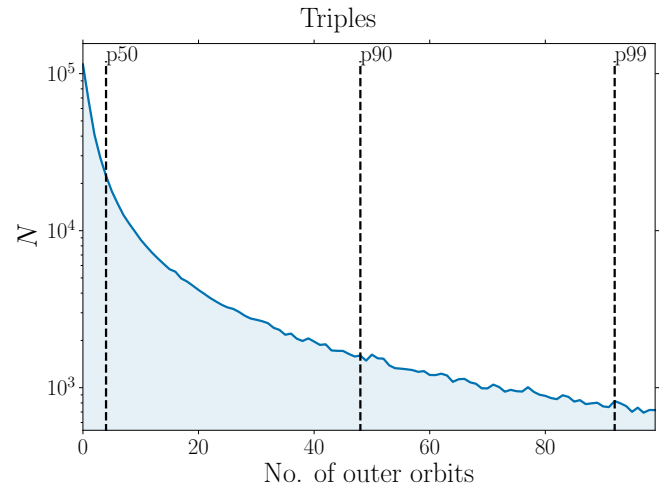


Figure 1. Plot of the number of outer orbits within which unstable triple-star systems become unbound. The dashed lines represent the 50th, the 90th and the 99th percentile values, which shows that the fraction of unstable systems that become unbound within 100 outer orbits decreases rapidly.

Newtonian mechanics predicts that a bound two-body system remains in a closed elliptical orbit indefinitely. On the other hand, the evolution of a three-body system can be, in general, chaotic and unpredictable. In many cases, minute changes in the initial parameters can manifest as substantial differences in evolution in secular timescales. Thus, we need to decide about how to quantify stability. We deem a triple system stable if it remains bound for 100 outer orbits and if the semimajor axes of both inner and outer orbits do not change by more than 10% of the initial value. The rationale for choosing 100 orbits is shown in Figure 1. The most unstable systems become unbound well before 100 outer orbits. There exist a small fraction of unstable systems which remain bound after 100 outer orbits, and the second criterion applies to these systems. The 10% threshold for semimajor axis change ensures that triple systems on the verge of becoming unstable are not erroneously classified as stable.

3 DATA SET AND INITIAL CONDITIONS

We generate initial conditions for hierarchical triple systems such that the parameter space is filled more or less uniformly. This is necessary to ensure good classification.

Moreover, to analyse the parameter space more thoroughly, we look at different parameter space slices, where one or more initial parameters are kept constant while others are varied. We perform three kinds of parameter space slices:

- Varied semimajor axes and masses, constant eccentricities and mutual inclinations (see Table 1).
- Varied semimajor axes and eccentricities, constant masses and mutual inclinations (see Table 2).
- Varied semimajor axes and mutual inclinations, constant masses and eccentricities (see Table 3).

We also limit our parameter ranges to remain in the triple-star system domain:

- $10^{-2} \leq q_{\text{in}} \leq 1$, $10^{-2} \leq q_{\text{out}} \leq 10^2$
- $10^{-4} < \alpha < 1$

Slice	e_{in}	e_{out}	i_{mut}
Fiducial	0.0	0.0	0.0
$i_{\text{mut}} = \pi/2$	0.0	0.0	$\pi/2$
$i_{\text{mut}} = \pi$	0.0	0.0	π
$e_{\text{out}} = 0.3$	0.0	0.3	0
$e_{\text{out}} = 0.6$	0.0	0.6	0
$e_{\text{in}} = 0.3$	0.3	0.0	0
$e_{\text{in}} = 0.6$	0.6	0.0	0

Table 1. Parameter space slices where α , q_{in} and q_{out} are varied, and other parameters are kept constant. The columns in the table show the constant values of these parameters in different slices.

Slice	q_{in}	q_{out}	i_{mut}
Fiducial	1.0	0.5	0.0
$i_{\text{mut}} = \pi/2$	1.0	0.5	$\pi/2$
$i_{\text{mut}} = \pi$	1.0	0.5	π
$q = 0.1, 0.818$	0.1	0.818	0.0
$q = 1, 9$	1.0	9.0	0.0
$q = 0.8, 0.111$	0.8	0.111	0.0

Table 2. Parameter space slices where α , e_{in} and e_{out} are varied, and other parameters are kept constant. The columns in the table show the constant values of these parameters in different slices.

Slice	q_{in}	q_{out}	e_{in}	e_{out}
Fiducial	1.0	0.5	0.0	0.0
$e_{\text{out}} = 0.3$	1.0	0.5	0.0	0.3
$e_{\text{out}} = 0.6$	1.0	0.5	0.0	0.6
$e_{\text{in}} = 0.3$	1.0	0.5	0.3	0.0
$e_{\text{in}} = 0.6$	1.0	0.5	0.6	0.0
$q = 0.1, 0.818$	0.1	0.818	0.0	0.0
$q = 1, 9$	1.0	9.0	0.0	0.0
$q = 0.8, 0.111$	0.8	0.111	0.0	0.0

Table 3. Parameter space slices where α and i_{mut} are varied, and other parameters are kept constant. The columns in the table show the constant values of these parameters in different slices.

- $0 \leq e_{\text{in}} < 1, 0 \leq e_{\text{out}} < 1$
- $0 \leq i_{\text{mut}} \leq \pi$.

4 UPDATED FORMULA

As mentioned previously, we attempt to improve on the previously existing and widely used stability criterion given by [Mardling & Aarseth \(2001\)](#). Before detailing our updated stability criterion, we mention the two stability criteria with which we compare our classification performances.

- Defining $Y = [a_{\text{out}}(1 - e_{\text{out}})]/[a_{\text{in}}(1 + e_{\text{in}})]$ [Eggleton & Kiseleva \(1995\)](#) (henceforth EK95) derived the following fitting formula for stability:

$$Y_{\text{crit}} = 1 + \frac{3.7}{q_{\text{out}}^{-1/3}} - \frac{2.2}{1 + q_{\text{out}}^{-1/3}} + \frac{1.4}{q_{\text{in}}^{-1/3}} \frac{q_{\text{out}}^{-1/3} - 1}{q_{\text{out}}^{-1/3} + 1}. \quad (1)$$

A hierarchical triple-star system is deemed ‘stable’ if $Y > Y_{\text{crit}}$ and ‘unstable’ if $Y < Y_{\text{crit}}$.

- The other criterion we will compare against is the semi-analytical, and more accurate, formula by [Mardling & Aarseth \(2001\)](#) (henceforth MA01):

$$\frac{R_{\text{p,crit}}}{a_{\text{in}}} = 2.8 \left[(1 + q_{\text{out}}) \frac{1 + e_{\text{out}}}{(1 - e_{\text{out}})^{1/2}} \right]^{2/5} \left(1 - \frac{0.3i_{\text{mut}}}{\pi} \right) \quad (2)$$

Here, $R_{\text{p}} = a_{\text{out}}(1 - e_{\text{out}})$ is the outer periastron distance and a triple system is deemed ‘stable’ if $R_{\text{p}} > R_{\text{p,crit}}$ and ‘unstable’ otherwise.

Finally, we present our stability criterion. After taking into account the dependencies on the initial parameters, we defined a new parameter \tilde{e}_{in} as follows:

$$\begin{aligned} e_{\text{in,max}} &= \sqrt{1 - \frac{5}{3} \cos^2 i_{\text{mut}}}; \\ e_{\text{in,avg}} &= 0.5e_{\text{in,max}}^2; \\ \tilde{e}_{\text{in}} &= \max(e_{\text{in}}, e_{\text{in,avg}}). \end{aligned} \quad (3)$$

The first equation is the quadrupole-order approximation for the maximum value of inner eccentricity due to LK oscillations. The second equation describes the *average* eccentricity during an orbit in the sense that the *time-averaged* separation for a single orbit is $\langle r_{\text{in}} \rangle = a_{\text{in}}(1 + e_{\text{in,avg}})$ (see [Stein & Elsner 1977](#)).

Our updated stability criterion is as follows:

$$\begin{aligned} \tilde{Y}_{\text{crit}} &= 2.4 \left[\frac{(1 + q_{\text{out}})}{(1 + \tilde{e}_{\text{in}})(1 - e_{\text{out}})^{1/2}} \right]^{2/5} \\ &\times \left[\left(\frac{1 - 0.2\tilde{e}_{\text{in}} + e_{\text{out}}}{8} \right) (\cos i_{\text{mut}} - 1) + 1 \right]. \end{aligned} \quad (4)$$

Here, \tilde{Y} is the same as Y with e_{in} replaced by \tilde{e}_{in} . The second term in the equation accounts for some of the complicated dependence on mutual inclination, whereas the first term is very similar to the MA01 formula with an additional \tilde{e}_{in} dependence.

The reasoning behind the choices for the dependencies in Equation 4 is detailed in the following sub-sections.

4.1 Eccentricity dependence

From our parameter space slices of eccentricities, we found that an additional dependence on e_{in} can better describe the classification boundary between stable and unstable systems. This is unlike the MA01 formula, which has no dependence on e_{in} .

Figures 2 and 3 illustrate the dependence of stability on both e_{in} and e_{out} . The dependence of Y_{crit} on e_{out} is the same as the MA01 factor $(1 - e_{\text{out}})^{-2/5}$, while the extra dependence on e_{in} is taken into consideration in Equation 4 through the factor $(1 + e_{\text{in}})^{-2/5}$. It should also be noted that Equation 4 works better for prograde orbits (Figure 2) than for retrograde orbits (Figure 3). Retrograde systems tend to have a stronger dependence on e_{in} for stability than prograde systems. Nonetheless, it is a notable improvement on previously existing stability criteria.

4.2 Mutual inclination dependence

The parameter space slices of mutual inclinations showed that the inclination dependence on stability is not linear. The ad-hoc inclination factor in the MA01 formula, $(1 - 0.3i_{\text{mut}}/\pi)$, is a good linear approximation but leaves room for improvement. In particular, systems with mutually highly inclined orbits (around $i_{\text{mut}} = \pi/2$) tend

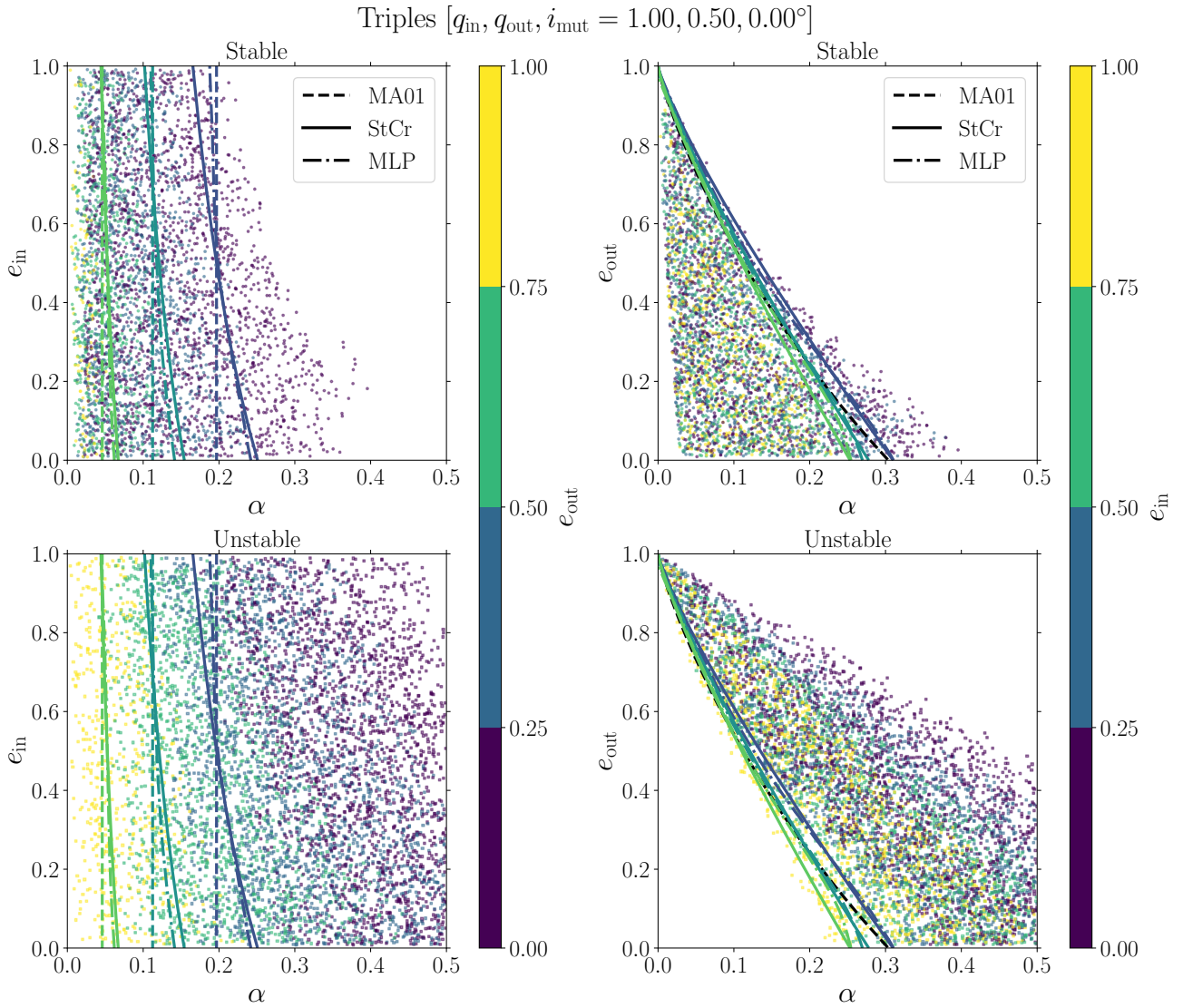


Figure 2. Plot showing a parameter space slice of varying α , e_{in} and e_{out} . The constant values of the other parameters are mentioned at the top. The left panel plots e_{in} vs α , while the right panel plots e_{out} vs α . The missing varied parameter is the colour axis in all panels. The top and bottom panels show the systems which remain stable and become unstable respectively from direct N -body simulations. The lines represent contours of the classification boundaries, with the legend labels ‘MA01’, ‘StCr’ and ‘MLP’ referring to the MA01 criterion, our updated stability criterion (Equation 4) and our MLP model respectively. The colours of the contour lines coincide with the transition values on the colour axes. The black lines are independent of the colour axis.

to be less stable than those with both less-inclined prograde and retrograde orbits. Moreover, retrograde orbits tend to be more stable than prograde orbits, which is also captured by the MA01 formula.

To account for the bowl-shaped depression in the stability classification boundary, we employed a trick used by [Grishin et al. \(2017\)](#). We replaced e_{in} by \tilde{e}_{in} , defined in Equation 3.

The motivation for doing this substitution is that the inner eccentricity, unlike the outer eccentricity, is not constant in the quadrupole-order approximation of LK oscillations. The e_{in} value changes the most for highly inclined orbits, and hence, replacing the initial value of e_{in} with a more average value can help to better characterise such systems.

Figures 4 and 5 represent the ‘bowl-shaped’ depressions of instability. Furthermore, the value of q_{out} also changes the inclination dependence. Equation 4 works best when q_{out} is high, i.e., the outer star’s mass is comparable or higher than the inner binary stars’ masses

(Figure 4). On the other hand, when q_{out} is low, mid-range retrograde orbits may be wrongly classified near the stability boundary (Figure 5).

4.3 Mass ratio dependence

Note that, just like the MA01 formula, Equation 4 has the same q_{out} dependence factor $(1 + q_{\text{out}})^{2/5}$ and no dependence on q_{in} . Our parameter space slices of mass ratios showed almost no dependence on q_{in} (except when mass ratios are very small, $\lesssim 0.1$). If we were to replace the quadrupole-order approximated expression for $e_{\text{in,max}}$ by the non-test particle limit formula presented by [Hamers \(2021\)](#), the slight dependence on q_{in} can be accounted for to some extent. However, we found that this replacement did not perform significantly better in classification whereas the expressions are significantly more complicated.

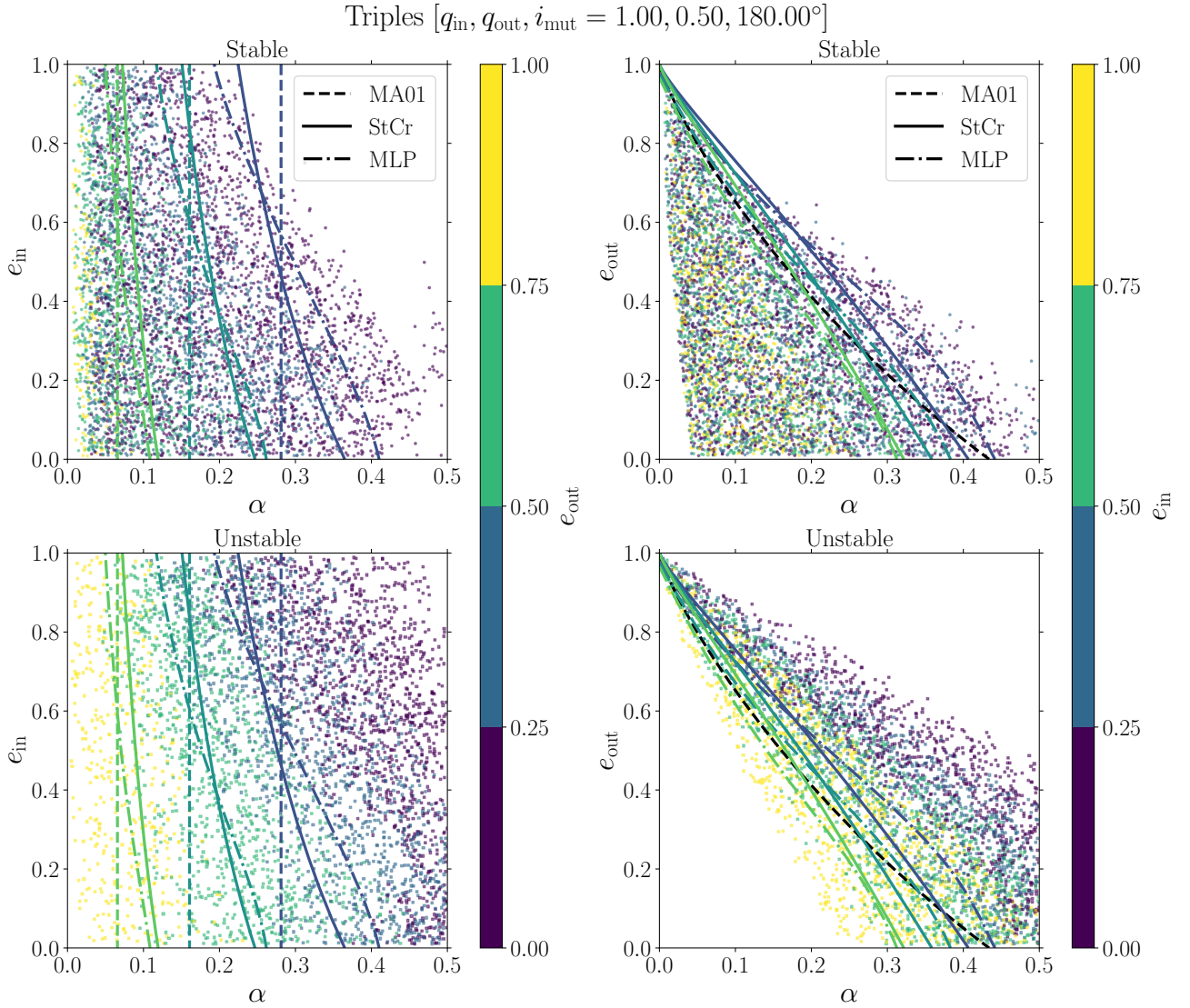


Figure 3. Plot similar to Figure 2, but showing a different parameter space slice. The changed constant values are mentioned at the top.

Figure 6 validates the above claims. The small dependence on q_{in} can be seen in both figures as a tail in the very-low mass ratio regime.

5 MACHINE LEARNING APPROACH

Machine learning (ML) classifiers are ubiquitous in the current era of computing. The basic premise of all ML algorithms is to learn from data to improve in classification or regression tasks. The results of such algorithms depend on the model parameters and hyper-parameters, which need to be tuned for reasonable performance.

5.1 Multi-layer perceptrons

An artificial neural network (ANN; McCulloch & Pitts 1943; for a review, see Hastie et al. 2009) is a supervised ML algorithm, which uses connected units (neurons), arranged in a series of layers, to perform classification tasks. Each neuron receives inputs from other neurons from the previous layer and provides outputs to the neurons in the following layer. The connection strengths between neurons are

controlled by weights. The output of a given neuron is the linear weighted sum of the inputs from the previous layer, which is then passed through an activation function ϕ before being input to the next layer. Thus, the output of the j th neuron is given as:

$$y_j = \phi \left(\sum_{i=0}^n w_{ij} x_i + b_j \right) \quad (5)$$

Here, \mathbf{x} are the inputs from the neurons from the previous layer and n is the number of such neurons. The parameters \mathbf{w} and \mathbf{b} are optimised during training. The network does this by minimising a pre-defined loss function, which depends on the consensus between the true classification labels and the predicted labels.

We specifically implement the simplest form of an ANN called a multi-layer perceptron (MLP; Rosenblatt 1958. MLPs are fully-connected ANNs, in the sense that every neuron in a given layer is connected to every neuron in the immediately adjacent layers. They consist of an input layer, one or more hidden layers and an output layer. Figure 7 shows a schematic of the MLP network we used for the classification of stable and unstable triple-star systems.

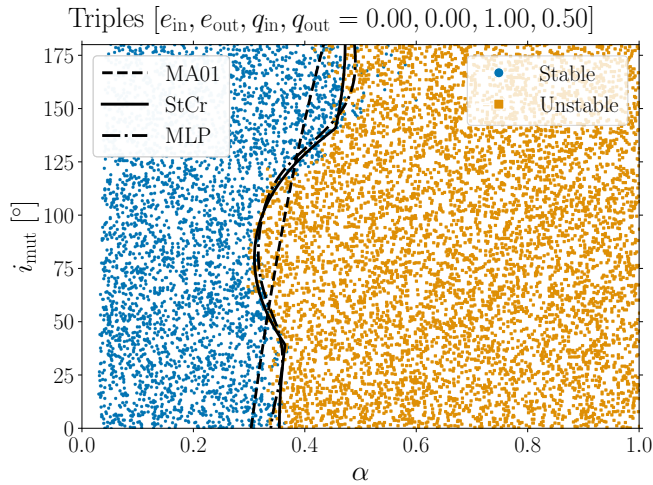


Figure 4. Plot showing a parameter space slice of varying α and i_{mut} . The constant values of the other parameters are mentioned at the top. The left and right panels show the systems which remain stable and become unstable respectively from direct N -body simulations. The lines represent the classification boundaries, with the legend labels ‘MA01’, ‘StCr’ and ‘MLP’ referring to the MA01 criterion, our updated stability criterion (Equation 4) and our MLP model respectively.

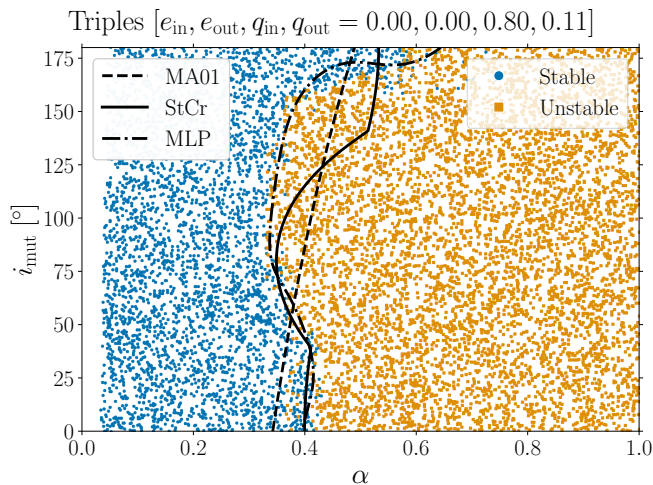


Figure 5. Plot similar to Figure 4, but shows a different parameter space slice. The changed constant values are mentioned at the top.

For the MLP classifier, we use an implementation provided by the `scikit-learn` (Pedregosa et al. 2011) package in Python.

5.2 Training and testing data sets

We generated 10^6 hierarchical triple-star systems whose initial conditions were sampled uniformly throughout our parameter space, with the parameter limits mentioned in Section 3. Besides these six parameters, we also sample the arguments of periaapsis and mean anomalies of both orbits uniformly. However, these values are not supplied to the MLP network as inputs. Since the data sparsely populated the six-dimensional space, we added a constraint to ensure that systems are sampled closer to the classification boundary. Additionally, we

disregarded systems whose N -body integration took longer than five hours. These made up 0.4% of our total sample.

To do this, we consider the MA01 formula $R_{p,\text{ratio}} = R_p/R_{p,\text{crit}}$ (Equation 2). If this ratio is greater than 1, a triple-star system is labelled ‘stable’, and vice-versa. However, since the formula does not have 100% accuracy, there is a range of values around 1 where systems can be classified incorrectly. We found that the range $0.3 \leq R_{p,\text{ratio}} \leq 2.0$ is the most ambiguous for classification. Thus, after sampling our triple systems, we eliminated any system whose $R_{p,\text{ratio}}$ value lies outside this range. This ensures that our training data, which lay within the range, is well suited for classification.

During classification, we use an 80:20 split of training and testing data. This, along with 5-fold cross-validation, was implemented to help validate the performance of the classifier.

5.3 Network architecture and hyper-parameters

We tried different network architectures and varied the hyper-parameters to arrive at the best-performing MLP model. The performance of a classifier refers to how well the model predicts the labels of previously unseen data – the test set. We chose our hyper-parameters by training a grid of MLP models, along with 5-fold cross-validation.

Our final model consists of 6 hidden layers of 50 neurons each (shown in Figure 7). Training a network of this size, with 10^6 training data points, takes about 30 minutes on 64 cores of an AMD EPYC 7742 CPU. The performance was found to be slightly worse with 4 or 5 hidden layers, and having 10 or 100 neurons in each layer worsened the classification substantially compared to having 50 neurons.

For optimisation, the network uses the *Adam solver* (Kingma & Ba 2014), which is a stochastic gradient descent algorithm. Finally, we use the *logistic* activation function $\phi(x) = 1/(1+e^{-x})$ for the neuron outputs. Although slower in implementation than the widely used *ReLU* (rectified linear unit) activation function $\phi(x) = \max(0, x)$, the logistic function performs slightly better.

Other hyper-parameters include:

- Batch size, which is the size of the mini-batches used for stochastic gradient descent. After experimenting with batch sizes of 200, 1000 and 5000, we chose 1000.
- L2 regularisation term, which is an additional term in the loss function that penalises the squares of the weights. If this penalty is too low, there is an increased risk of over-fitting, and vice-versa. After experimenting with values of 10^{-2} , 10^{-3} and 10^{-4} , we chose 10^{-3} .
- Initial learning rate, which controls the step-size of updating the weights and biases after each iteration. If it is too low, the optimiser takes a very long time to converge to the minimum of the loss function; if it is too high, the minimum can be skipped. After experimenting with values of 10^{-2} , 10^{-3} and 10^{-4} , we chose 10^{-2} .

6 RESULTS AND COMPARISON

To quantify the effectiveness of any classification algorithm, we need to consider a few quantities. Some of these include:

- Overall score: The fraction of systems which are classified correctly i.e., the ‘stable’ and ‘unstable’ systems are indeed stable and unstable respectively from direct N -body simulations.
- False stable (*FS*) systems: The number of truly unstable (from N -body simulations) systems that the model predicts as ‘stable’. Similarly, we can define true stable (*TS*) systems.

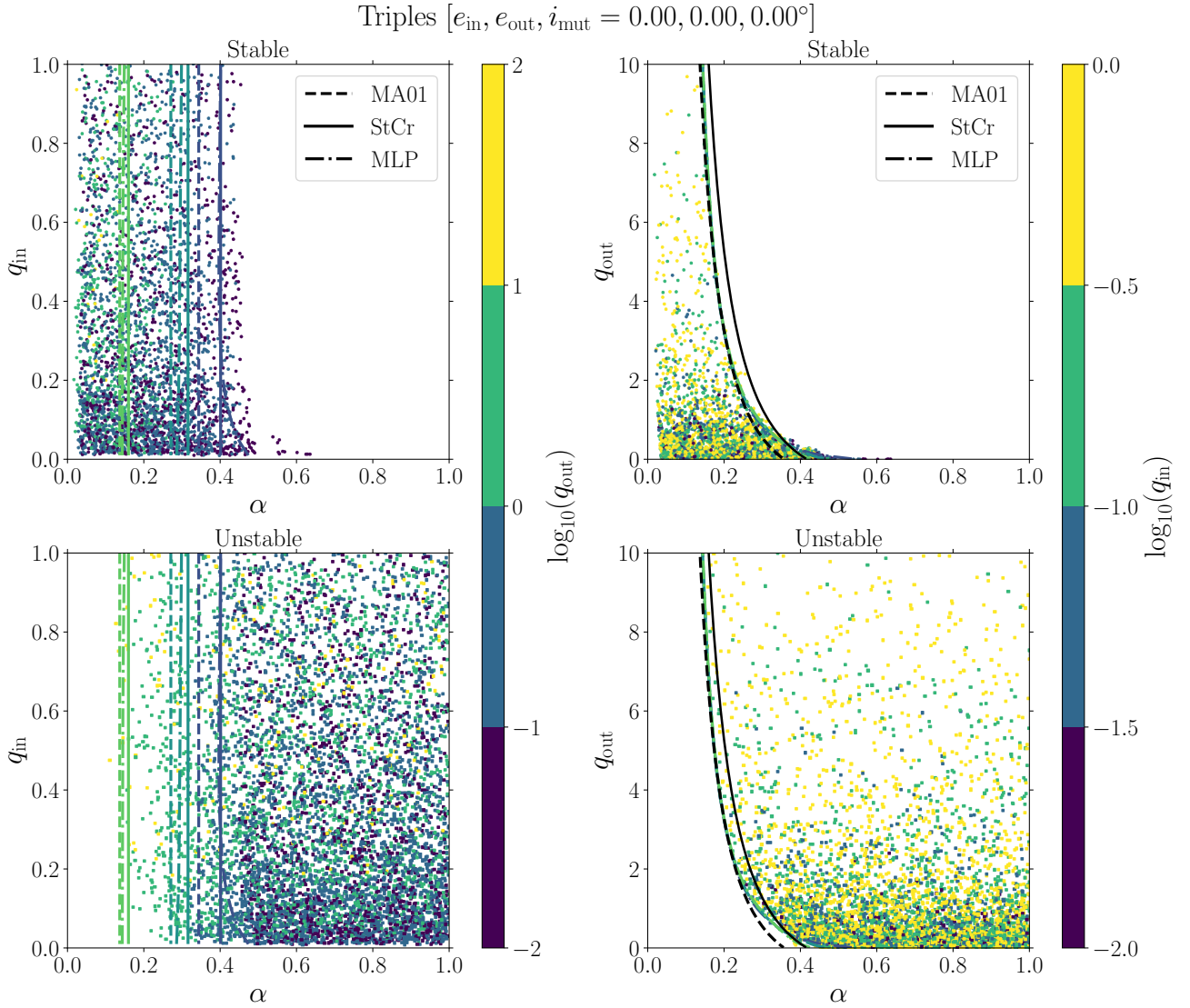


Figure 6. Plot showing a parameter space slice of varying α , q_{in} and q_{out} . The constant values of the other parameters are mentioned at the top. The left panel plots q_{in} vs α , while the right panel plots q_{out} vs α . The missing varied parameter is the colour axis in all panels. The top and bottom panels show the systems which remain stable and become unstable respectively from direct N -body simulations. The lines represent contours of the classification boundaries, with the legend labels ‘MA01’, ‘StCr’ and ‘MLP’ referring to the MA01 criterion, our updated stability criterion (Equation 4) and our MLP model respectively. The colours of the contour lines coincide with the transition values on the colour axes. The black lines are independent of the colour axis.

- **False unstable (FU) systems:** The number of truly stable (from N -body simulations) systems that the model predicts as ‘unstable’. Similarly, we can define true unstable (TU) systems.

- **Precision:** The ratio of correctly classified stable (unstable) systems to the total number of systems classified as ‘stable’ (‘unstable’): $P_{\text{stable}} = TS/(TS + FS)$ and $P_{\text{unstable}} = TU/(TU + FU)$. It quantifies validity of the classification.

- **Recall:** The ratio of correctly classified stable (unstable) systems to the total number of truly stable (unstable) systems: $R_{\text{stable}} = TS/(TS + FU)$ and $R_{\text{unstable}} = TU/(TU + FS)$. It quantifies completeness of the classification.

Table 4 shows the comparison of scores, precisions and recalls of EK95, MA01, our updated Equation 4 and our MLP model from Section 5. It is evident that both our methods score better than the previous studies, and that the MLP model performs the best in classification. It is important to note that these scores can vary depending

Classifier	Score	P_{stable}	P_{unstable}	R_{stable}	R_{unstable}
EK95	0.86	0.96	0.81	0.68	0.98
MA01	0.90	0.92	0.90	0.81	0.96
StCr	0.93	0.93	0.92	0.85	0.96
MLP	0.95	0.93	0.96	0.92	0.96

Table 4. Overall scores, precisions P and recalls R for the different classifiers we compare with. The labels ‘StCr’ and ‘MLP’ refer to our updated stability criterion (Equation 4) and our MLP model respectively.

on the range of sampled parameter space. In our case, we sampled ‘close’ to the MA01 classification boundary line as described in Section 5.

We also show the false stable and unstable rates for the three parameter space slices (see Section 3) in Figures 8, 9 and 10 respec-

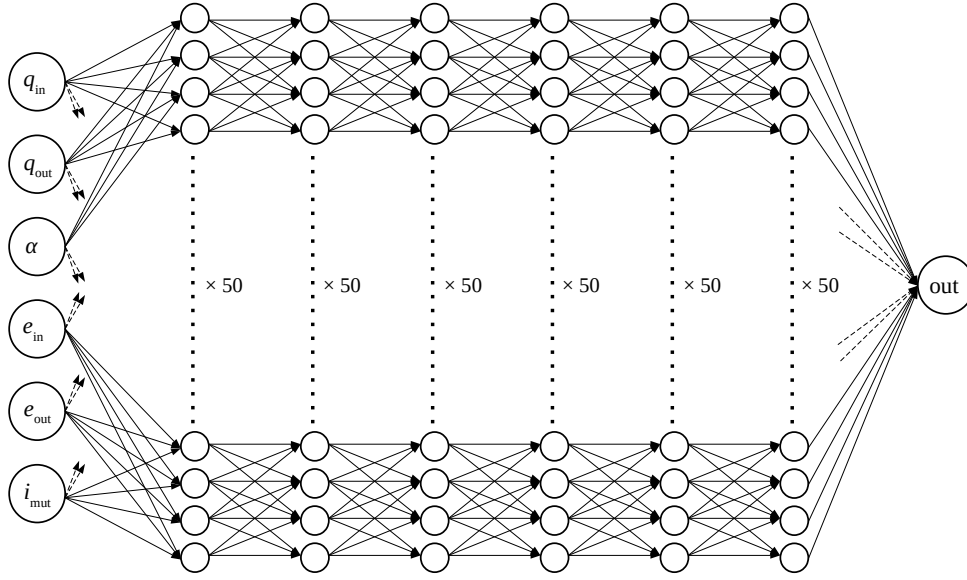


Figure 7. Schematic of the MLP architecture used for classification. Every neuron in a given layer is connected to every neuron in the adjacent layers. The input layer has 6 neurons (q_{in} , q_{out} , α , e_{in} , e_{out} , i_{mut}), the output layer has one neuron (value ranges from 0 for ‘stable’ to 1 for ‘unstable’), and the six hidden layers have 50 neurons each.

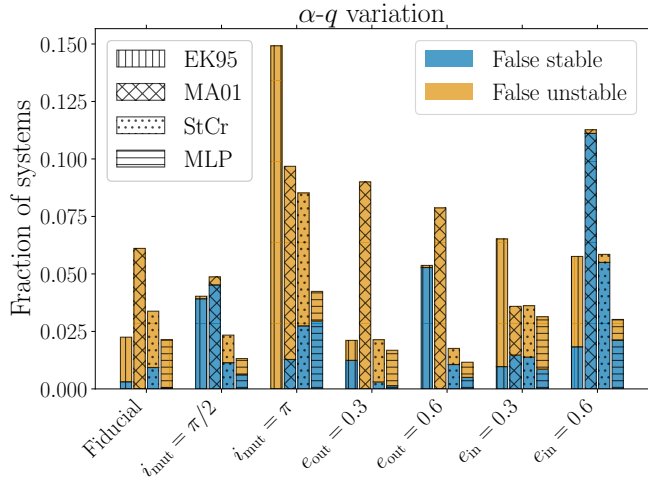


Figure 8. Bar chart illustrating the total fraction of ‘false stable’ and ‘false unstable’ systems (defined in text) in the parameter space slice of varying α , q_{in} and q_{out} . The x -axis labels refer to the constant values described in Table 1. The legend labels ‘StCr’ and ‘MLP’ refer to our updated stability criterion (Equation 4) and our MLP model respectively.

tively. Again, both our methods perform better than EK95 and MA01 in all parameter space slices, with the MLP model being better in most cases. The figures indicate that the parameter space slices of retrograde orbits ($i_{mut} = \pi$) have the highest misclassification rates. High e_{in} values can also lead to less efficient classification. On the other hand, parameter space slices with high q_{out} seem to have the best classification rates.

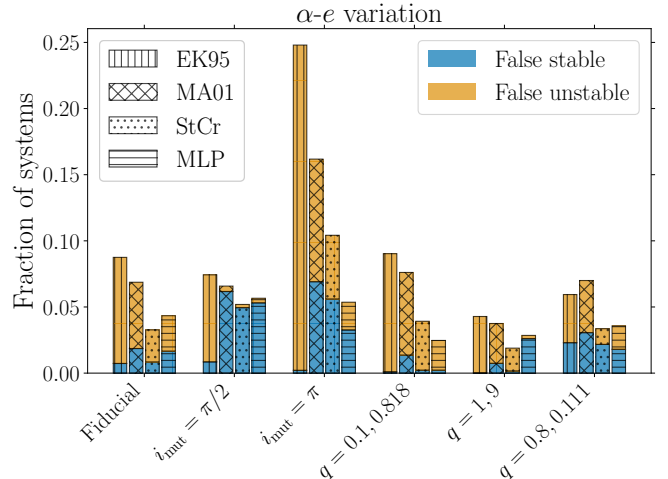


Figure 9. Plot similar to Figure 8, but in the parameter space slice of varying α , e_{in} and e_{out} .

7 DISCUSSION

We reiterate that our defining criterion for stability (see Section 2) is not absolute and that the accuracy of our classification would vary if we were to employ a different defining criterion. Moreover, our integration time of 100 outer orbits does not fully capture the instability of those systems that become unbound much later on. For example, [Mardling \(2008\)](#) demonstrated that the trajectory of a triple close to the stability boundary can diverge from another almost identical triple with slightly different initial conditions even after 100 outer orbits (see Figure 3.7). Our additional criterion that the inner and outer semimajor axes must not change more than 10% accounts

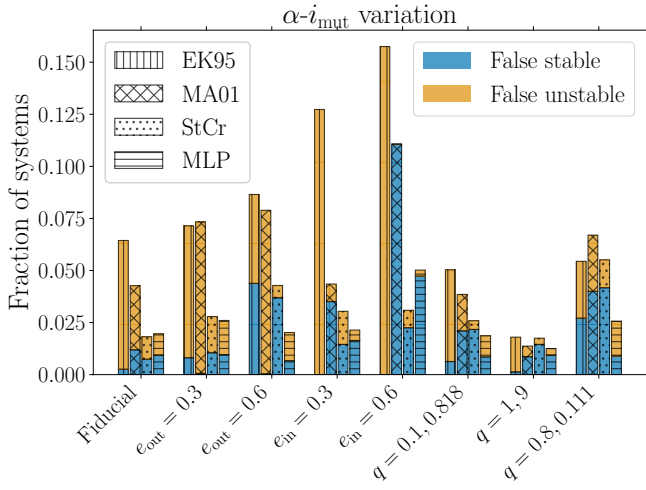


Figure 10. Plot similar to Figure 8, but in the parameter space slice of varying α and i_{mut} .

for some of these unstable systems, but not all. This assumption is reasonable since hierarchical triples that become unstable undergo non-periodic, i.e., persistent transfer of energy between the inner and outer orbits. Since the semimajor axes are inversely proportional to the energies of the respective orbits, any significant change in their values would indicate that the triple is on the verge of becoming unbound.

It is worth noting that, very recently, [Lalande & Trani \(2022\)](#) also presented a machine learning approach to determine the stability of hierarchical triples. They employ a convolutional neural network (CNN), with a time series of orbital parameters as the training data, to perform the classification. This is unlike our classification which depends only on the *initial* values of the parameters, which makes our MLP model simpler and faster to use. They also assume equal masses, whereas we consider the dependence on mass ratios in our analysis. Finally, we highlight that an algebraic criterion like Equation 4 can be more useful than an ML classifier in understanding the physical dependencies on the initial parameters.

Stability criteria have also been used to classify hierarchical quadruple-star systems. Many studies, including [Hamers et al. \(2021\)](#) and [Vynatheya & Hamers \(2022\)](#), applied the MA01 criterion to quadruples by considering them as two ‘approximate’ triple systems. For example, in a 2+2 quadruple system, one of the two inner binaries can be approximated as a single-star companion to the other inner binary. Hence, applying the triple stability criterion twice (one with each inner binary) yields an effective quadruple-star stability criterion. A similar procedure can be applied on a 3+1 quadruple by approximating the innermost binary as a single star and plugging in the triple stability criterion to the two ‘nested’ triples. Nevertheless, as shown by our preliminary findings, this process does not always predict the stability of the quadruple accurately, especially in cases where the mutual inclinations of the orbits are significant. To overcome this, we are working on a quadruple stability criterion as well ([Vynatheya et al. in prep](#)) to analyse this problem in greater detail.

8 CONCLUSION

We presented an algebraic criterion to classify hierarchical triple-star systems based on their dynamical stability. This formula is an

improved version of the widely used stability criterion of [Mardling & Aarseth \(2001\)](#) (MA01). We also performed the same classification using a fully connected neural network - a multilayer perceptron (MLP). Our labelled training data of 10^6 triples are generated by direct N -body simulations of triple-star systems using the N -body code MSTAR ([Rantala et al. 2020](#)). The main summary and results of the paper are presented in the following points:

- Our updated formula, Equation 4, adds a dependence on inner orbital eccentricity e_{in} which is absent in the MA01 formula. It also has a more complicated dependence on mutual orbital inclination i_{mut} , an improvement over the inclination dependence of MA01 described by an ad-hoc inclination factor.
- Similar to the MA01 criterion, Equation 4 does not have an explicit dependence on inner mass ratio q_{in} . This is mostly justified, the only exception being the regime where both inner and outer mass ratios are very low ($\lesssim 0.1$).
- Equation 4 performs better than MA01 in all parameter space slices considered and has an overall classification score of 93%. The precisions of stable and unstable systems are 93% and 92% respectively, while the recalls are 85% and 96% respectively. In general, the classification is least effective for retrograde orbits and high inner eccentricities.
- Our MLP model is a neural network of six hidden layers of 50 neurons each. It performs even better than Equation 4 in classification and has an overall classification score of 95%. The precisions of stable and unstable systems are 93% and 96% respectively, while the recalls are 92% and 96% respectively.
- The classification works best in the parameter ranges of mass ratios $10^{-2} \leq q_{\text{in}} \leq 1$, $10^{-2} \leq q_{\text{out}} \leq 10^2$ and semimajor axis ratio $10^{-4} < \alpha < 1$. This range corresponds to a major fraction of hierarchical triple-star systems.
- Our MLP model is publicly available on Github [in the form of a simple Python script](#).

ACKNOWLEDGEMENTS

A. S. H. thanks the Max Planck Society for support through a Max Planck Research Group. Funding for the Stellar Astrophysics Centre is provided by The Danish National Research Foundation (Grant agreement no.: DNRFF106).

DATA AVAILABILITY

The data underlying this article will be shared upon reasonable request to the corresponding author.

REFERENCES

- Antonini F., Chatterjee S., Rodriguez C. L., Morscher M., Pattabiraman B., Kalogera V., Rasio F. A., 2016, *ApJ*, **816**, 65
- Chirikov B. V., 1979, *Phys. Rep.*, **52**, 263
- Eggleton P., Kiseleva L., 1995, *ApJ*, **455**, 640
- Fragione G., Loeb A., 2019, *MNRAS*, **486**, 4443
- Grishin E., Perets H. B., Zenati Y., Michaely E., 2017, *MNRAS*, **466**, 276
- Hamers A. S., 2021, *MNRAS*, **500**, 3481
- Hamers A. S., Fragione G., Neunteufel P., Kocsis B., 2021, *MNRAS*, **506**, 5345
- Hastie T., Tibshirani R., Friedman J., 2009, The elements of statistical learning: data mining, inference and prediction, 2 edn. Springer, <http://www-stat.stanford.edu/~tibs/ElemStatLearn/>

- Kingma D., Ba J., 2014, International Conference on Learning Representations
- Kozai Y., 1962, *AJ*, **67**, 591
- Lalande F., Trani A. A., 2022, arXiv e-prints, p. [arXiv:2206.12402](https://arxiv.org/abs/2206.12402)
- Lidov M. L., 1962, *Planet. Space Sci.*, **9**, 719
- Mardling R. A., 2008, in Aarseth S. J., Tout C. A., Mardling R. A., eds., Vol. 760, The Cambridge N-Body Lectures. p. 59, [doi:10.1007/978-1-4020-8431-7_3](https://doi.org/10.1007/978-1-4020-8431-7_3)
- Mardling R. A., 2013, *MNRAS*, **435**, 2187
- Mardling R., Aarseth S., 1999, Dynamics and Stability of Three-Body Systems. Springer Netherlands, Dordrecht, pp 385–392, [doi:10.1007/978-94-015-9221-5_38](https://doi.org/10.1007/978-94-015-9221-5_38)
- Mardling R. A., Aarseth S. J., 2001, *MNRAS*, **321**, 398
- McCulloch W. S., Pitts W., 1943, The bulletin of mathematical biophysics, **5**, 115
- Moe M., Di Stefano R., 2017, *ApJS*, **230**, 15
- Naoz S., 2016, *ARA&A*, **54**, 441
- Pedregosa F., et al., 2011, Journal of Machine Learning Research, **12**, 2825
- Rantala A., Pihajoki P., Mannerkoski M., Johansson P. H., Naab T., 2020, *MNRAS*, **492**, 4131
- Rosenblatt F., 1958, Psychological Review, pp 65–386
- Stein S. K., Elsner T., 1977, *Mathematics Magazine*, **50**, 160
- Vynatheya P., Hamers A. S., 2022, *ApJ*, **926**, 195
- von Zeipel H., 1910, *Astronomische Nachrichten*, **183**, 345

APPENDIX A: USING OUR MLP MODEL

Using our MLP model is simple. We have uploaded a code on GitHub [🔗](#) to ensure easy access.

The first step is to install the scikit-learn package (if not already available) using the following terminal command:

```
pip3 install scikit-learn
```

After changing to the repository directory, the python3 module is run on the terminal as follows:

```
python3 mlp_classify.py -qi 1.0 -qo 0.5 -al 0.2
-ei 0.0 -eo 0.0 -im 0.0
```

Here, the arguments qi , qo , al , ei , eo and im refer to q_{in} , q_{out} , α , e_{in} , e_{out} and i_{mut} respectively. The parameter ranges should be restricted to the values given in Section 3 for optimal results.

It is also possible to import the MLP classifier to another custom python3 script. The input parameters can also be numpy arrays, as shown in the sample script below:

```
import numpy as np
from mlp_classify import mlp_classifier

# generate initial numpy arrays qi, qo, al, ei, eo, im

mlp_pfile = "./mlp_model_best.pkl"

mlp_stable = mlp_classifier(mlp_pfile, qi, qo,
                           al, ei, eo, im)

# returns True if stable, False if unstable
```

This paper has been typeset from a \TeX/L\AA\TeX file prepared by the author.